COVER PAGE

Bibliographical reference

Prediction Method for Wind-Induced Vegetation Noise, Karl Bolin, Acta Acustica **vol. 95** (Number 4), 2009, pp. 607-619

DOI

https://doi.org/10.3813/AAA.918189

ACTA ACUSTICA UNITED WITH ACUSTICA
Vol. 95 (2009) 607 – 619

DOI 10.3813/AAA.918189

Prediction Method for Wind-Induced Vegetation Noise

Karl Bolin
KTH – Linné FLOW centre / The Marcus Wallenberg Laboratory, Teknikringen 8,
100 44 Stockholm, Sweden. kbolin@kth.se

Summary
This article examines the sound generated when the wind interacts with vegetation. A wind field model has been coupled to a new method for predicting sound from vegetation. This includes predictions from coniferous, deciduous and leafless trees. The proposed prediction method and an earlier model have been compared with measurements which show improved agreement, in particular in the region below 1 kHz. Comparisons between five measurement sites and predictions show satisfactory agreement for wind speeds up to 8.5 m/s. Fluctuations in the vegetation noise level due to wind turbulence can also be accurately estimated.

PACS no. 43.28.Fp, 43.28.Py

1. Introduction

Wind turbines are an emerging man-made noise source. Turbines will increase both in number and in size, as signing states of the Kyoto protocol need to fulfill their promises to decrease greenhouse gases. Noise disturbances from wind turbine plants are thus a growing problem in many rural regions. Therefore the need for correct estimations of the perceived annoyance is increasing. Even wind turbine sound levels as low as 40 dB (A-weighed) of noise could be perceived as annoying [1]. This might be explained by some characteristics different from other sources namely amplitude modulations caused by blades passing the tower and the feeling of an unending noise source [2] compared to the transient noise from traffic and aircraft. Today's large wind turbines (2–5 MW) are often pitch-regulated fixed rotor speed wind turbines. The main noise source of these turbines is the aero-acoustic broadband noise from the wing tips. The increased wind turbine size also means that turbines are located in forested areas. This is because the deteriorated wind conditions close to the tree tops are not as severe at hub heights (80–120 m) compared to turbine heights (25 m) 25 years ago [3].

Concerning the extended periods when wind turbines produce noise these occur when the wind speed is above cut in wind speed (3–5 m/s) and below cut off (∼20 m/s). The audibility of the wind turbine depends not only on the wind turbine noise level but also on the background noise level. Therefore the ambient noise levels are important when the impact from wind turbine noise is assessed. One of the main natural ambient noise sources is sound from vegetation. The wind triggers the onset of this sound [4]. This sound could mask the wind turbine noise as shown in [5]. This natural noise source is common in rural and recreational areas and is also of broadband character. Therefore it is suitable to mask the wind turbine noise. Furthermore the vegetation could conceal the wind turbine. This has been shown to decrease the annoyance peceived by nearby residents [1].

The British assessment method [6] allows for turbine sound level 5 dB higher than measured background noise levels ($L_{A90,10min}$) at different wind speeds. This procedure will hopefully result in optimized power output without causing disturbances to nearby residents. Naturally, extensive measurements for all seasons have to be performed in every wind turbine project, a method can prove both time-consuming and expensive. Therefore this article aims at presenting a prediction model of one of the most common natural sounds, that from vegetation. This could be used to estimate the potential effect of making vegetation noise on wind turbine noise.

Although sound generated by vegetation is perceived daily by a large part of the population, little research has been conducted in the field. Measurements of all-year vegetation noise were reported in [7] but no prediction model was presented. Fégeant proposed a semi-empirical analytical prediction model of vegetation noise in [4] and [8] for different tree species and vegetation geometries. This analysis was validated for steady wind speeds. Further work by Fégeant [9] stressed the importance of wind turbulence causing fluctuations in the level of vegetation noise. These local variations could deteriorate the masking effect by making the wind turbine noise audible although it is masked most of the time. The work performed by Fégeant, however impressive, shows some limitations; leafless deciduous trees were not modeled and field measurements have been performed at wind speeds of 7 m/s and below.

Received 23 September 2008,
accepted 8 March 2009.

Verification of the model above these conditions is considered necessary if reliable predictions are to be produced. Furthermore, it is problematic to couple the expressions in [4] to turbulence models. This could be avoided if the vegetation sound sources are treated at discrete points.

This article presents turbulence models and vertical wind speed profiles depending on the atmospheric conditions coupled to the vegetation noise model. Furthermore, measurements of fluctuating vegetation noise and comparison with simulation results are presented. The objectives of this article are to improve the Fégeant model, especially in the low frequency region which is important to the masking issue as wind turbine noise is usually of this character. A further objective is to incorporate the fluctuations due to wind turbulence into the model. A new model is suggested to estimate sound from deciduous trees without foliage. The analytical expressions from [4] have been replaced by discrete equivalents, better suited to deal with complex and diversified terrain, wind turbulence and changing atmospheric conditions. Comparisons between the two models and new measurements are also presented. Measurements of vegetation noise have been performed at seven locations at higher wind speeds than reported in previous studies.

2. Wind models

The noise from vegetation is induced by the wind. Consequently correct wind characteristics in different vegetation types are important to the vegetation noise issue. The wind can be separated into an average part, stationary in magnitude and direction, and a time-varying turbulent part. Both these components will influence noise emission from vegetation. Wind velocity models in and around vegetation have received considerable attention in the field of boundary layer meteorological research, among others those of Panovsky and Dutton [10] and Kaimal and Finnigan [11]. The part of the atmosphere closest to the ground is called the surface layer. It is this region that is of interest in the current application as tree heights are normally lower than the height of the surface layer.

Wind profiles depends on the ground configuration, modeled by the roughness length, z_0. Vertical speed profiles are also influenced by the atmospheric conditions. This has not been taken into account in [4] but has been included in this paper. These atmospheric states are usually classified into stable, neutral and convective conditions. A stable atmosphere occurs when the temperature gradient $\mathrm{d}T(z)/\mathrm{d}z = \theta(z) > \theta_{\text{adiabatic}} \approx 0.01$ [K/m] [11] and thus the air at lower heights has higher density than the air above, thereby reducing the vertical wind motion. For example, this condition arises on clear nights when the ground is colder than the air and results in large variations of wind speed with respect to height. A neutral atmosphere is characterized by a temperature gradient $\theta(z) \approx \theta_{\text{adiabatic}}$ and is often used as a reference case as it is the intermediate state between the other two conditions. A convective or unstable condition occurs when $\theta(z) < \theta_{\text{adiabatic}}$.

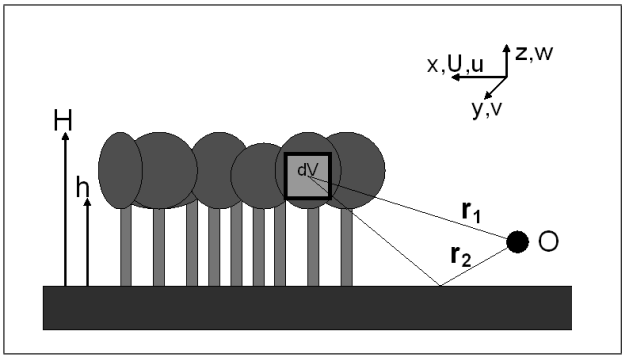

Figure 1. Geometry of vegetation with tree height H, trunk space height h, volume element dV, propagation paths $\mathbf{r_1}$ and $\mathbf{r_2}$ to observer position $\mathbf{O}$. In the upper right corner the Cartesian coordinates (x, y, z) where x corresponds to the mean wind direction with wind speed $\mathbf{U}$ and turbulence u, y is the horizontal direction perpendicular to x and z is the vertical directions with their respective wind components v and w.

For example, this happens on warm sunny days when the heated ground causes large vertical wind motions and turbulence. This mixing of air results in wind speeds that change less with respect to height than in neutral or stable atmospheres.

2.1. Average wind

The mean wind is defined as the wind velocity over a ten-minute interval [3]. The coordinate system is chosen such that x coordinate is aligned with the mean wind direction and the mean wind speed is denoted by U, y is the horizontal coordinate perpendicular to x and z is the vertical coordinate positive upwards with respective turbulence components u, v, w. These quantities are shown in Figure 1.

2.1.1. Flow inside forests

In the paper of Harmann and Finnigan [12] the vertical velocity profile, $U(z)$, inside vegetation canopies is modeled by an exponential function of the height

$$U(z) = U_H \exp\left(\frac{\beta(z-H)}{l}\right), \tag{1}$$

where H is the tree height, U_H is the wind speed at the tree tops and β depends on the roughness length as well as the atmospheric stability [12]. In this paper the roughness length is assumed constant inside forests and average values from [12] yields $\beta = 0.37$ for stable, 0.31 for neutral and 0.27 for unstable atmospheric conditions. The mixing length, l, is defined as

$$l = 2L_c\beta^3, \tag{2}$$

where the canopy penetration depth, L_c, depends on the drag coefficient, C_d, and the leaf area index I_{la} [$\mathrm{m^2/m^2}$]. L_c can be approximated [12] by

$$L_c = (C_d I_{la})^{-1} \approx 4H/I_{la}. \tag{3}$$

The leaf area index is the one-sided leaf area per unit ground area. This depends on growing conditions (sparse or dense stand, access to light etc.).

This wind speed profile model is validated inside both deciduous and coniferous forests [12] and is also assumed valid inside forest edges when the wind's direction is from the forest [4]. Equation (1) shows good resemblance to measured wind profiles in the upper parts of the foliages [12]. This is important as this region will generate a large part of the noise due to higher wind speeds. The local wind speed maximum observed [13] in the trunk space is not accounted for. This is, however considered of relatively low importance as the stems are probably minor noise generators.

2.1.2. Flow at forest edges

As stated in the earlier section the forest wind profile is assumed valid inside forest edges when the wind's direction is from the forest [4]. In the case when the wind propagates from an open field into foliage the wind speed decelerates and the velocity profile changes. A new equilibrium state is reached at the distance between $2.1H$ and $3.6H$ inside the foliage according to large eddy simulations, field measurements and wind-tunnel experiments [14].

The vertical velocity profile is influenced by the upwind ground configuration. This dependence is partly modeled by the roughness length z_0 [10]. In farmland areas this parameter varies between 0.1 m for winter conditions and 0.6 m in summertime and grows to 1 m inside forests. The vertical velocity profile depends on both the roughness length and the atmospheric conditions. This is modeled by Panofsky and Dutton [10] as

$$U(z) = \frac{u_*}{k_a}\left[\ln\frac{z}{z_0} - \psi_m\left(\frac{z}{L}\right)\right], \tag{4}$$

where $k_a = 0.4$ is the von Karman constant, ψ_m accounts for the atmospheric stability and values from [15] are used for unstable conditions, in neutral conditions ψ_m=0 and for stable conditions $\psi_m = -5z/L$ [10]. The Monin-Obukhov length, L, depends primarily on the vertical heat flux at the surface and the friction velocity. In this article the value of L has been determined from Figure 6.6 in [10] and depends on the Turner class and the roughness length. The Turner class describes the atmospheric stability and has been determined in accordance with the procedure described in [10].

The wind speed is gradually reduced when the wind propagates from open fields into vegetation. This attenuation depends on the leaf area density D_{la} (m^2/m^3) of vegetation sources [4] where equation (5) was shown to give good agreement to measured profiles by Raynor [13]

$$U(x) = U_0 e^{-\varsigma D_{la} x} \tag{5}$$

where U_0 is the wind speed at the forest edge, x is the distance to the forest edge in the average wind direction and the dimensionless horizontal attenuation coefficient ς = 0.05 is used [4]. The leaf area density is the total one-sided leaf area per unit of ground surface and unit height. As shown in [4] increased leaf area density causes decreased winds within the foliage and the noise generation is therefore balanced by decreasing wind speeds. Values of D_{la} are given in [16], [17] and [18] for deciduous trees and [19] for coniferous trees. The leaf area index, I_{la}, in equation (3) can be calculated by integrating the leaf area density in the vertical direction.

When combining equation (4) and equation (5) the average wind speed in forest edges when the wind direction is from the open field, at shelterbelts and also at single trees is described by

$$U(z, x) = \frac{u_*}{k_a}\left[\ln\frac{z}{z_0} - \psi_m\left(\frac{z}{L}\right)\right] e^{-\varsigma I x}. \tag{6}$$

Although the vertical velocity profile transition above the canopies has been studied [11] the transition within the foliage seems to be relatively unknown. However, as the velocity profile transition is shown to be of marginal importance to the resulting sound level [4] the area from the edge to $x = 2H$ is assumed to have the velocity profile from equation (6) and the velocity profile at $x > 2H$ is modeled according to equation (1).

The wind profile will therefore be discontinuous at $x = 2H$ expect when $z = H$ where the wind speed $U(2H, H)$ from equation (6) is set equal to $U(H)$ in equation (1). This simplification could be excluded if large eddy simulations [14] are used. This is however considered beyond the scope of the present work as the suggested approximation yields satisfactory acoustic predictions as shown in [4]. It is furthermore shown [4] that if the observer is poside the forest the vegetation at a distance further than $2H$ from the edge can be neglected.

2.2. Wind turbulence

Fluctuations in vegetation noise could introduce short periods when the wind turbine noise could be audible even though it is masked most of the time. Turbulence in and around vegetation has been attracting attention from several researchers ([11, 20, 21, 22]). The turbulence effect on vegetation noise was examined in [9] where Fégeant derived a Gaussian distributed probability distribution of sound pressure levels in small vegetation geometries based on the assumption of moderate turbulence intensities, uniform wind speed in the vegetation and central limit theorem. The standard deviation, σ_{Lp}, of the sound pressure level L_p was estimated by

$$\sigma_{Lp} = \frac{20 \cdot 2\chi}{ln(10)} \cdot i_u, \tag{7}$$

where χ is a wind speed coefficient [4] and i_u is the wind turbulence intensity in the mean wind direction.

The work in [9], although innovative, contained assumptions of moderate turbulence intensities, $i_u = \sigma_u/U$, $i_v \ll i_u$ and $i_w \ll i_u < 1$, conditions that are sometimes fulfilled in open terrain, but not inside forests [11].

The wind speed was assumed to be varying only in time but not in space; therefore it is not valid for arbitrary

vegetation types but only for those with small extension where this assumption holds. Furthermore turbulence was restricted to the component parallel to the mean wind direction, not taking into account components perpendicular to the wind direction. It is the purpose of the present paper to provide a method to estimate fluctuations of vegetation noise in arbitrary vegetation geometries. This has been implemented by coupling wind field simulations [23] with time- and space-varying wind speeds to a vegetation noise model.

The non-deterministic nature of wind turbulence can be modeled as a stochastic process correlated in space and time. In order to extract time series, wind field simulations [23] have been used. This model has originally been used to estimate wind fluctuations around wind turbines. In this article this method has simulated the wind field inside vegetation and has been used as input to the vegetation noise model. A brief description of the wind field simulation and the parameters chosen in this paper is shown below. For further details see [23]. The wind turbulence temporal characteristics are described by the power spectrum, S, depending on the frequency, f. In this paper the Kaimal et al [24] spectra have been used. The spectra for the velocity components u, v and w are

$$\begin{aligned} nS_u(n)/u_*^2 &= 105\, f/(1+33f)^{5/3}, \\ nS_v(n)/u_*^2 &= 17\, f/(1+9.5f)^{5/3}, \\ nS_w(n)/u_*^2 &= 2\, f/(1+5.3f)^{5/3}, \end{aligned} \tag{8}$$

where $n\ (= fz/U)$ is the nondimensional frequency. The wind field method uses a sheared spectral tensor [25] for atmospheric surface layer turbulence multiplied by Gaussian stochastic variables and FFT to create a mesh of space and time correlated wind speeds at different points. The objective of the method is to resemble the second-order statistics i.e. variances, cross-spectra etc. which should be sufficient for the vegetation noise application. Then the turbulent mesh can be propagated across the discrete region containing vegetation as seen in Figure 2 (2D example).

The canopy's movements lag in time with respect to the wind speed. The prolonged effect on the vegetation noise, t_{veg}, should depend on the wind speed. A quasi-stationary vegetation noise model is assumed valid. Combination of the steady state vegetation noise model with a turbulent wind field requires that $t_{veg} < \Delta t$ where Δt is the time steps. This condition must be satisfied in order to avoid coupling between the noise from adjacent time steps due to the inertia of the vegetation. Time steps of 5 s are chosen as input to the vegetation noise model. This is considered a sufficiently large step as the canopy movement induced by a strong gust followed by low wind speed would be severely reduced after 5 s. The time step is chosen from a qualitative discussion instead of from measured quantities, which is regrettable. This simplification is used because measurements to quantify this parameter could not be acquired. Such measurements should include a sudden drop in the wind speed which rarely occurs in the field measurements. Wind tunnel measurements with fast changes in wind speed could also be used to estimate this parameter. However, these can not capture the inertial movement unless complete trees can be inserted into the tunnel. Furthermore the inertial movement of trees would depend on tree species, H, I_{la} and other environmental variables and would therefore be problematic to investigate.

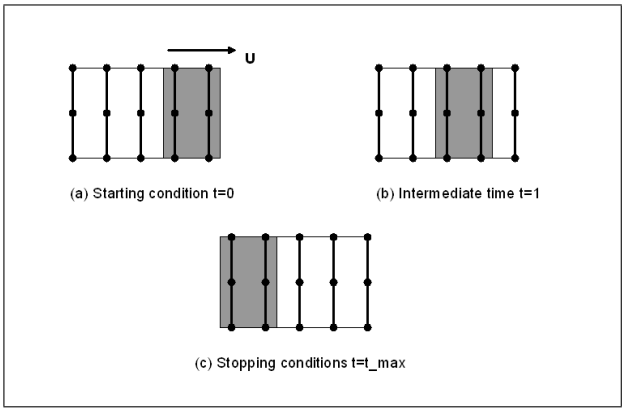

Figure 2. Wind speeds are calculated for every point (•) in the discrete plane, the vegetation is in the shaded area. The wind speed simulation starts as shown in (a), then the mesh propagate in the **U** direction as shown in (b) to the final state (c).

3. Vegetation noise

The physical mechanisms generating sound in trees are of varying origins in the cases of leafed, leafless deciduous and coniferous trees. In the leafed state, the dominating rustling sound at frequencies around 4 kHz is generated by contacts between leaves in the foliage [4]. A pink noise component was added in [4] to model the mechanical impact sound when canopy elements collide with each other and by vortex shedding around branches and twigs. In [4] Fégeant proposed a single sound generating mechanism by conifers from vortex shedding around needles. This is however questionable as the measured spectra show frequency components that could hardly be explained by this hypothesis. The low frequency parts of the spectra should be explained by the same low frequency sound generation mechanisms as in the deciduous species. Regarding the noise from leafless deciduous vegetation the rustling sou nd should be removed from the sound spectrum.

3.1. Fégeant's model

The semi-empirical analytical model developed by Fégeant [4] and [8] is to the author's knowledge the most complete prediction method of vegetation noise published. The effective acoustic pressure was calculated by a volume integral

$$p_{eff}^2(f) = \frac{\rho c}{4\pi} \iiint_V \delta W(f, \mathbf{r}) J(f, \mathbf{r})\, \mathrm{d}V, \tag{9}$$

where f is the frequency, $\mathbf{r}$ is the vector from the source to the receiver, ρ is the air density, c the sound speed, δW the

sound power emitted by volume element dV and $J(f, \mathbf{r})$ the propagation factor.

The function $J(f, \mathbf{r})$ shown in equation (10) represents the propagation of a spherical sound source along the rays $\mathbf{r}_1$ and $\mathbf{r}_2$ shown in Figure 1. It is expressed by

$$J(f, \mathbf{r}) = \left| \frac{e^{-\alpha r_1}}{r_1} + R\frac{e^{-\alpha r_2}}{r_2} \right|^2, \quad (10)$$

where α is the attenuation coefficient calculated according to ISO 9613 [26] (disregarding phase [4]). R is the ground reflection coefficient calculated as described by Delany and Bazeley in [27] with ground impedance values, Z, calculated with flow-resistance values from [28].

The sound power, δW, from volume element dV is calculated by

$$\delta W(f, \mathbf{r}) = U^{2\chi} A \cdot D_{la}(\mathbf{r}) \Gamma(f), \quad (11)$$

where χ is a wind speed coefficient and A is a radiation constant with the unit depending on χ. These parameters are described in detail in [4, 8]. The dimensionless frequency spectra $\Gamma(f)$ are fitted to sound power measurements performed in a reverberant room. These are separated for coniferous and deciduous species. In the coniferous case it is described by

$$\Gamma_c(f) = e^{-\lambda_1 (lgf/f_c)^2}. \quad (12)$$

λ_1 determines the width of the spectrum and is 10 for pine and 15 for spruce. The Strouhal frequency, f_c, is expressed by

$$f_c = St\frac{U}{d_n}, \quad (13)$$

with the Strouhal number set to $St = 0.2$ and d_n is the needle diameter 1.3 mm for pine and 1.0 mm for spruce.

For the deciduous species the spectrum is given by

$$\Gamma_d(f) = C_1 f^{-1} + C_2 e^{-C_3 (f - f_d)^2 / f_d^2}. \quad (14)$$

The coefficients $C_{1,2,3}$ and f_d are described in [8]. The first term in this expression represents a pink noise term which describes the low frequency sound emission and the second part in the expression originates from the rustling leaves.

3.2. Proposed model

3.2.1. Discrete model

The Fégeant model is analytical, and not well suited to combine with the nondeterministic nature of wind turbulence which is preferably modeled by a random process. To circumvent this predicament a discrete vegetation noise model is proposed. This could be combined with a stochastic turbulence model in order to evaluate the fluctuations of vegetation sound caused by variations of wind speed. The emitted power ΔW_{nop} from the volume element ΔV_{nop}, where (n, o, p) represent discrete positions in the (x, y, z) space can be written as

$$\Delta W_{nop}(f, \mathbf{r}) = C_R I(\mathbf{r})\, M_{nop}^{2\chi} \cdot \Gamma(f) \quad (15)$$

where C_R (Wm^{-3}) is the species-dependent radiation constant. The wind speed U_{nop} is replaced by the Mach number $M_{nop} = U_{nop}/c$ to ensure that the radiation constant C_R has a constant unit. C_R can be compared to the radiation constant A in equation (11) with unit depending on χ. The expression $C_R = A \cdot c^{2\chi}$ gives C_R values of $6.4 \cdot 10^{-6}$ for birch, $4.0 \cdot 10^{-5}$ for aspen, $1.8 \cdot 10^{-6}$ for oak, $2.4 \cdot 10^{-5}$ for pine and $1.4 \cdot 10^{-5}$ for spruce with A values from Fégeant [8]. The discretization of the sound pressure in equation (9) is

$$p_{eff}^2(f) = \frac{\rho c}{4\pi} \sum_{n=1}^{N} \sum_{o=1}^{O} \sum_{p=1}^{P} J(f, \mathbf{r}) \cdot \Delta W_{nop}(f, \mathbf{r}) \Delta V, \quad (16)$$

where $\Delta V = \Delta x \Delta y \Delta z$, the step size is chosen to be $\Delta x = \Delta y = 2\Delta z = 2$ m. The propagation factor, $J(f, \mathbf{r})$, is calculated from the midpoint of each element. N, O and P are the maximum values of the discrete space in $x-$, $y-$ and $z-$ direction. Numerical testing shows that the predicted sound pressure levels converge within ± 0.5 dB for the above mentioned step sizes compared to step sizes of $\Delta x = \Delta y = \Delta z = 0.5$ m. This convergence is observed for extended sources and compact sources, for example forests and single trees respectively. The wind field from section 2.2 is then inserted into equation (16) and thereby the time varying sound pressure is calculated.

The number of calculations can be reduced by replacing the 3D wind field with a 2D field parallel to the ground. With this simplification variations in the wind field's vertical direction are neglected and thereby the summation over the $z-$direction in equation (16) can be uncoupled from the summations in the horizontal directions. equation (17) shows the separated summation in the vertical direction.

$$\Delta W_{no}(f, \mathbf{r}) = \sum_{p=1}^{P} \Delta W_{nop}(f, \mathbf{r}). \quad (17)$$

This equation is then used to calculate the acoustic power at each integer wind speed from 1 to 25 m/s and the values are stored. The turbulent wind speeds are noninteger values and therefore linear averages of equation (17) from the two nearest integer wind speeds are calculated at each time step and inserted into equation (18). The sound pressure can thereby be estimated at each time step as

$$p_{eff}^2(f) = \frac{\rho c}{4\pi} \sum_{n=1}^{N} \sum_{o=1}^{O} J_{no}(f, \mathbf{r}) \cdot \quad \Delta W_{no}(f, \mathbf{r}) \Delta V, \quad (18)$$

where $J(f, \mathbf{r})$ has been replaced by propagation from a reference plane $\mathbf{r} = (x, y, (H + h)/2)$ to decrease the number of computations in the algorithm. The relatively simple sound propagation calculation used in the present method [26, 29] could be improved by implementing the

sound propagation model proposed by Tunick [30]. This would enable the model to include vegetation from longer distances. This would probably improve the predictions. However, the model considers o nly vegetation at relatively short distances because it was shown in [4] to contribute most of the generated sound.

3.2.2. Deleafed deciduous spectrum

Although innovative, the work of Fégeant [4] and [8] shows some limitations. The most obvious inadequacy can be observed in the deciduous trees at leafless conditions when $\lim_{I_{la}\to 0} \delta W = 0$. Since the hibernated state will be the condition for large parts of the year it is considered important that a prediction method for these trees exists if all-year predictions of vegetation noise are to be performed. Although wind tunnel measurements of a leafless birch were reported in [31] no model was presented. The wind-tunnel-canal's extension was 0.7×0.7 m. Therefore this procedure could not capture the movement of the entire tree and could consequently miss canopy movements important to the noise generation. Results from field measurements are instead used in this paper to produce a noise prediction model for leafless deciduous trees. This model uses data from two field measurements (site 5 and 7 in section 4) to estimate model parameters.

Not only the noise emission is changed with no leaves but also the flow through the canopies is altered. Compared to the foliaged state, leafless conditions increase the porosity of the canopies and the wind speeds.

The mean wind speed is approximately doubled but the wind profile in leafless conditions changes little compared to the fully leafed profile [32]. The windward speed reduction at forest edges is assumed to be similar to the leafed state equation (5) but the leaf area density is replaced by the biomass density, D_{bm} and the attenuation coefficient ς_{dl} is fitted to reach the equilibrium state in leafless conditions [14] as can be seen in equation (19) instead of the fully leafed equilibrium state equation (5)

$$U(x) = U_0 \mathrm{e}^{-\varsigma_{dl} D_{bm} x}, \quad \varsigma_{dl} = \frac{\varsigma D_{la}}{D_{bm} ln(2)} = 0.43. \qquad (19)$$

Compared to ς the leafless attenuation coefficient is larger. This is however compensated for by lower values of D_{bm} than of D_{la}. equation (19) yields faster wind speeds in the canopies resulting in higher Reynolds numbers and larger motions in the canopies, thereby increasing the number of collisions. Analogous to the D_{la} in [4] a higher biomass density should be balanced by decreased wind speed in the canopy. However, the drag coefficient is lower

herefore this effect should be less significant in the leafless state.

The main sound sources from leafless trees are assumed to be mechanically induced vibrations from collisions between canopy elements and dipole sources from vortex shedding when the wind flows around the branches and twigs. In the leafless case the amount of noise generated from a tree should depend on the biomass m_b in branches and twigs. The biomass depends on several circumstances

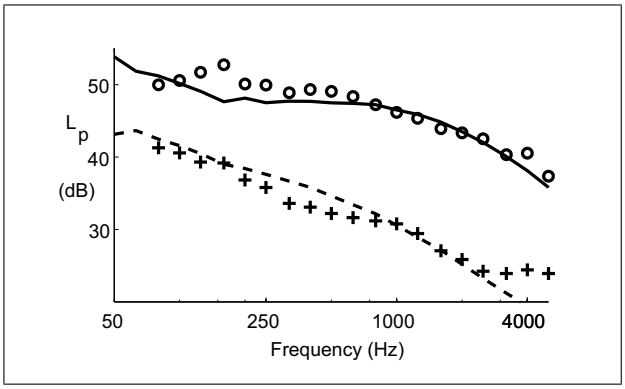

Figure 3. Third octave band noise spectra in dB of leafless trees from measurement Site 5 (+) and prediction (- - -) at wind speed of 3.2 m/s. Measurement from site 6 (∘) and prediction (—) at $U = 5.7$ m/s.

for example, the tree species, growing conditions of the trees and soil type[33]. The biomass can be estimated by biomass functions for aspen in [34], birch in [33] and alder in [35] and is approximately proportional to H^3 for these three species. To the author's knowledge the distribution of biomass within the canopy has not been investigated. Therefore the biomass is assumed to be uniformly distributed in the canopy volume, $V_c \propto H^3$, and therefore the biomass density can be calculated by $D_{bm} = m_b/V_c$. For birch, aspen and alder D_{bm} =0.74, 0.25 and 0.22 [kg/m^3] respectively. In the leafless case the sound power is not proportional to I_{la} as in equation (11) and is replaced by D_{bm} this yields

$$\Delta W_{nop}(f, \mathbf{r})) = C_R D_{bm}(\mathbf{r})\, M_{nop}^{2\chi} \cdot \Gamma_{dl}(f), \qquad (20)$$

where $C_R = 6 \cdot 10^{-5}$ [W/m^{3}kg].

The spectrum of leafless trees should be different compared to trees with leafs. The sound generating mechanism from rustling leafs should disappear. This is shown in Figure 3 where the characteristic frequency component around 4 kHz [4] for leafed trees has dissolved.

The low frequency part of the leafed spectrum may also change because the dynamics of a leafless tree should be different from a tree with leaves. Two main sound generating mechanisms for leafless trees are proposed in this paper. The first should be a low frequency part from colliding canopy elements. The second mechanism should be vortex shedding around twigs. This part should be analogous to the needle sound in equation (12) but with the average twig diameter instead of the needle diametere two sources are included in the leafless spectrum shown in equation (21)

$$\Gamma_{dl}(f) = C_4 f^{-2} + \mathrm{e}^{-\lambda_{dl}(lg f/f_{dl})^2}, \quad f_{dl} = St\frac{U}{d_{dl}}, \qquad (21)$$

where $C_4 = 6.0 \cdot 10^4$ [s^2] is a constant and $\lambda_{dl} = 3$ is a parameter that describes the width of the spectrum and is larger than in the coniferous needle diameter. This seems reasonable as the twig diameter distribution should be wider than the needle diameter distribution. The term

Table I. Parameters of the coniferous spectrum in equation (22).

Species	C_c	λ_2	d_2 [m]
Pine	100	0.50	0.03
Spruce	100	0.16	0.20

f^{-1} in equation (14) has been replaced by f^{-2} as a steeper slope seems to fit the data in Figure 3 better. At the second line d_{dl}=5 mm could be coupled to the

ge diameter of the branches and twigs. The central limit theorem states that the sum of a large number of random variables is normally distributed. The wind speeds within the canopy as well as twig diameters vary. Therefore, it is reasonable to assume that the spectrum is Gaussian distributed. This is analogous to the conclusion in [4] concerning the spectrum from vortex shedding around needles. The values of the coefficients are acquired from least squares approximations of measurements from site 5 and 6 shown in Figure 3.

The wind speed dependence of noise from leafless trees is shown in Figure 4. The data from site 5 and site 6 in the figure is adjusted to an average sound pressure level of 45 dB at $U = 5$ m/s. The wind speed coefficient χ was set to 1.5 as this value corresponds to a regression line with an inclination of $29log(u)$ [8] seen in Figure 4.

3.2.3. Coniferous spectrum

The coniferous spectrum derived by Fégeant in [4] has a single sound generating mechanism, the dipole source created when the air flows around the needles. Therefore predictions in Figure 5 show large estimation errors in the low frequency domain. It is believed that these low frequency sound levels could be explained by structural vibrations caused when the canopy elements collide and by vortex shedding from branches and twigs. Therefore, a term is added to equation (12) as shown in equation (22)

$$\begin{aligned} \Gamma_c(f) &= \mathrm{e}^{-\lambda_1 (lgf/f_c)^2} + C_c \mathrm{e}^{-\lambda_2 (lgf/f_2)^2}, \\ f_2 &= St\frac{U}{d_2}, \end{aligned} \tag{22}$$

where the coefficients λ_1 and f_c are acquired from equation (12), C_c, λ_2 and d_2 are species-dependent parameters estimated by least squares approximation of the measurements in Figure 5. The values for pine and spruce are shown in Table I. Compared to the deciduous spectrum where a pink noise term is added to account for the low frequency component a term similar to the sound from needles is chosen in the coniferous spectrum. The low frequency components, especially for pine, have higher wind speed coefficient than the high frequencies as can be seen in Figure 5. This discrepancy is elegantly compensated by the second term in equation (22) by increasing center frequencies instead of introducing a frequency dependent wind speed coefficient.

At very high wind speeds the proposed model would underestimate the low frequency region since the frequency

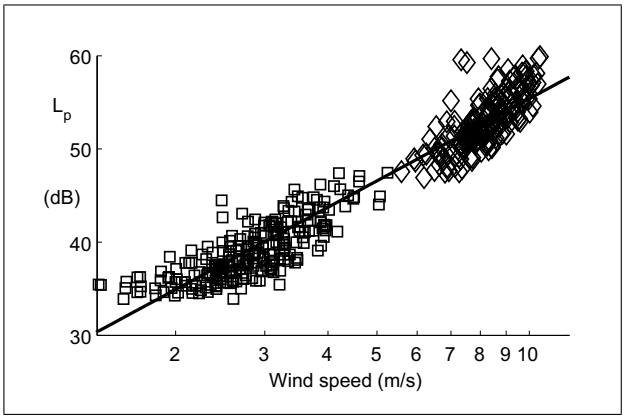

Figure 4. Scatter plot of the corrected emission peak levels (□) data obtained from site 5; (⋄) data obtained from site 6. The regression line (—) for the sound pressure is $26 + 29log(u)$.

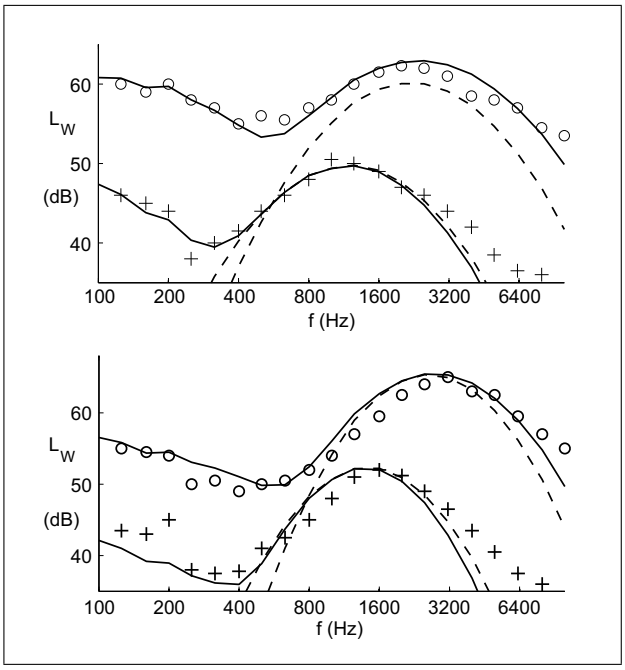

Figure 5. Wind tunnel measurements of the acoustic power in third octave band noise spectra from [4]. The figure shows coniferous species, wind speed 6.3 m/s, lower curves, and 11.5 m/s, upper curves. (o) Shows measurements, (—) predictions by new model and (- - -) predictions by Fégeant model.

top at f_2 would be shifted into the audible region. However, with the chosen parameters this peak would be at 20 Hz with a lowest corresponding wind speed of 0.2 km/s, and is therefore considered of academic interest. Unfortunately the values of d_2 cannot be coupled to any physically relevant diameter as in the case of the needle generated source term. This deficiency is considered excused as the spectrum shows improved accuracy in the low frequency region compared to Fégeant's spectrum. Furthermore, the sound generating mechanisms in the low frequency region, e.g. contact noise between canopy elements, are not fully understood and consequently difficult to model accurately. The evergreen coniferous trees will show smaller seasonal

variations in the sound spectrum and are therefore I_{la} is assumed constant over different seasons.

3.3. Spectral comparison between the Fégeant model and the proposed model

To compare measurements and predictions by Fégeant to the suggested model in an unbiased procedure some factors have been considered. Firstly, Fégeant used some of his measurement sites for parameter calibration; these are disregarded as they might bias the comparison. Secondly different tree species and wind speeds have been evaluated to give results with general validity. Therefore, this section presents measurements and predictions reported in [31] which are compared to the proposed mode

he ground configurations are assumed to be grass and the microphone is at 1.4 m above the ground in all measurements. The meteorological parameters are not specified in [31]. Therefore, temperatures of 20°C and relative humidities of 70% have been assumed in the simulations with the new model.

Edge of mixed species: This measurement location was a forest edge, labeled site 5 in [31]. The microphone was placed 40 m from the edge. The sound levels at this site are estimated with higher accuracy by the new model, as can be seen in Figure 6, especially in the low frequency region. The Fégeant model underestimates the sound level at 100 Hz by 18 dB compared to the new estimation where the error is 7 dB. The large error at low frequency noise could either be explained by vegetation noise from sources at larger distances which are not modeled or by other b ackground noise sources.

Edge of spruces: The site, labeled site 7 in [31], consisted of mainly spruces with two oak trees with 4 m foliage diameter close to the microphone. The spectrum in Figure 7 shows a typical conifer vegetation source with a frequency peak around 400 Hz. The new model shows higher accuracy than the Fégeant model, particularly in the low frequency region.

From the comparisons shown above it is evident that the new model predicts the low frequency sound generation by vegetation better than the model suggested by Fégeant. The effect of this improvement could be considered minor when estimating the total A-weighed sound pressure level. However, when the masking by vegetation noise on wind turbine noise is examined the consequence of this change could be significant. This is because the frequency spectrum from wind turbines [36] is usually dominated by low frequencies as can be seen in Figure 6.

4. Measurements

One aim of this paper is to measure the sound generated by vegetation at higher wind speeds than documented before. Another objective is to quantify the fluctuations due to turbulence. Furthermore, measurements of deciduous trees during the hibernated season are necessary to describe the noise generated in this state.

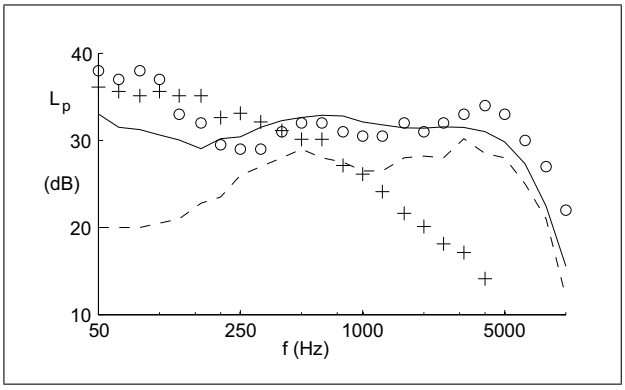

Figure 6. Sound pressure level in third octave bands at U = 4.4 m/s. (∘) measurement, (—) prediction by present method, (- - -) prediction by Fégeant for site 5 in [31]. Source spectrum from a 2 MW wind turbine at (+) from [36].

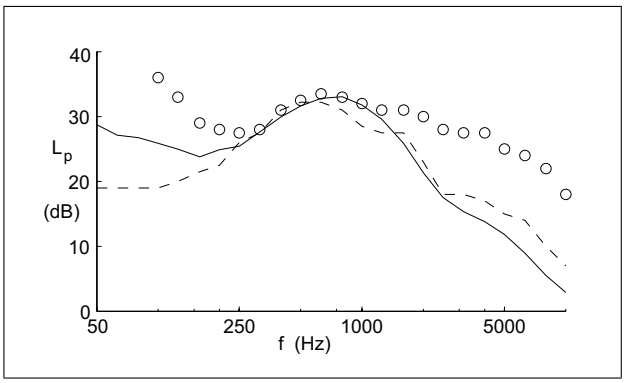

Figure 7. Sound pressure level in third octave bands at U = 2.5 m/s. (∘) measurement, (—) prediction by present method, (- - -) prediction by Fégeant for site 7 in [31].

Measurements were conducted in accordance to the procedure described in ISO 1996 [37]. The measurement setup consisted of a cup anemometer mounted on either a 6 m pole or 10 m pole, and a weather station registering humidity and temperature placed at 1 m height. The sound measurement equipment consisted of 1/2" microphones at 1.2 m height above ground connected to a digital analyzer SONY PC216Ax at site 1–3 and to a sound card Digigram VXpocket440 and a computer (Fujitsu Siemens lifebook S7110) at site 4–7. In order to decrease the noise produced when air flows on the microphone's protective grid and wind turbulence, referred to as pseudo-noise, the microphones were protected by a foam windscreen 10 cm in diameter. The damping produced by the protection is corrected in the analysis of the measurements. A high pass filter with a cutoff frequency of 23 Hz was used at sites 4–7 to improve the dynamics of the measurements by reducing the pseudo-noise. In these locations the anemometer was mounted at 6 m height and the wind speed extrapolated at 10 m height by equation (4) as the anemometer was placed in the open field at these measurements. Recordings were performed in the frequency range from 43.2 Hz to 8.9 kHz with a sampling frequency of 48 kHz at site 1–3 and sampling frequency 22.05 kHz at site 4–7.

4.1. Description of sites

When choosing measurement locations some main aspects have been taken into consideration. The first and most important factor is the absence of other noise sources (primarily traffic and aircraft noise). It is also favorable if sites have vegetation sources with uniform tree species and tree height. Unfortunately the cup anemometer overestimates wind speeds at high turbulence intensities [11]. Therefore no measurements well inside the vegetation have been performed. All measurement locations except site 3 fulfill the first condition. At that location a wind turbine Vestas 52 was situated 0.8 km downwind from the measurement location.

The geometries and microphone positions can be seen in Figure 8. Two sites (site 5 and 6) have been used for parameter calibration of the leafless model and two sites (site 4 and 7) investigate how the leafless predictions correspond to outdoor measurements. Site 5 and 6 were chosen as reference sites because the wind speed scatter plots, Figure 4, were separated but without large space between the series. Measurements have also been performed at higher wind speeds compared to earlier measurements; this was considered important in order to verify the model in these conditions.

In Table II the main characteristics of the measurement sites are shown and in Table III the meteorological parameters are shown. As only one anemometer is used no wind speed profile could be measured. Instead, the roughness length has been estimated from the turbulence intensities in Table IV. Comparisons between these values and Table 6.2 in [10] show that the roughness length has a reasonable magnitude. Deviations from the tabled values are seen at site 5 and 6 with underestimation at the former and overestimation at the latter location. The procedure to estimate roughness length from turbulence statistics might be questionable. However, as noted in [11] z_0 changes with altitude. At low heights the roughness length is determined by the terrain a short distance upwind compared to at higher altitudes where this distance increases. Therefore the tabled values in [10] are considered as guidelines rather than fixed values. Furthermore, the fluctuating noise simulations should be fairly compared to the measurements and this would not be the case if the measured and simulated wind series are very different.

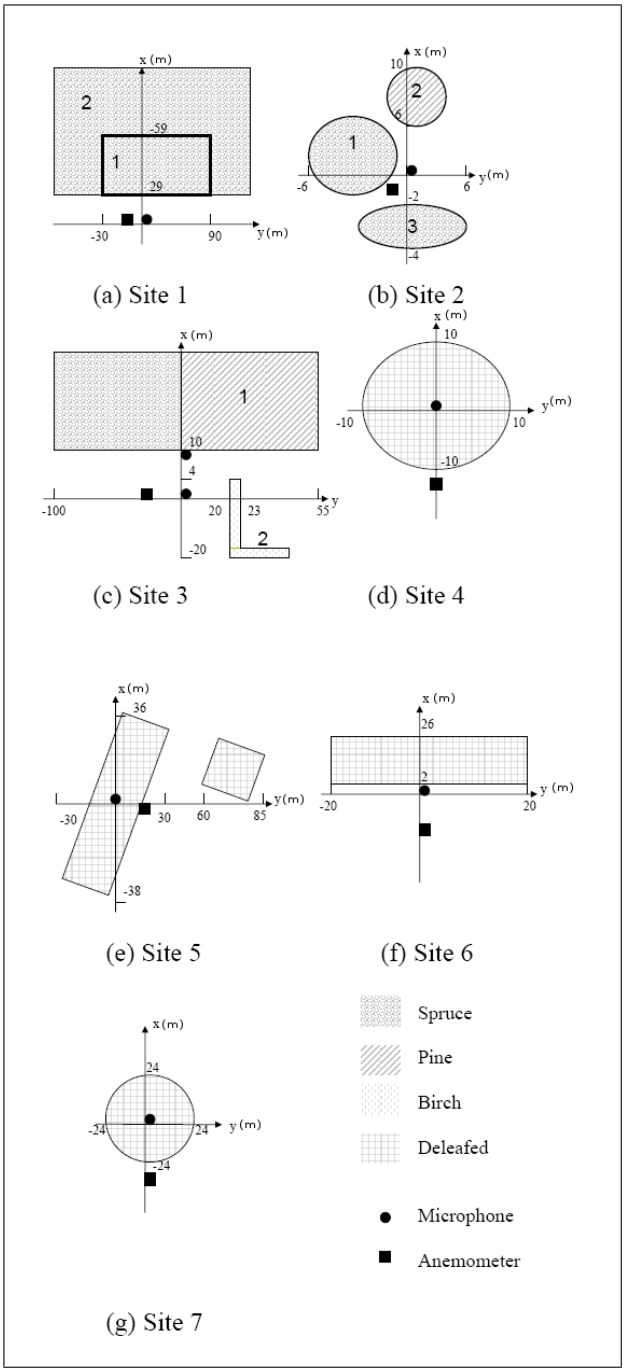

Figure 8. Sites geometries, microphone and anemometer positions.

Site 1 The measurement equipment was mounted at a forest edge consisting of spruces of mixed height.

Site 2 This location was dominated by a spruce and a pine. In the upward wind direction there was a shrubbery of junipers. The ground was covered with grass. The microphone and anemometer were placed a small distance from the spruce.

Site 3 This site is an upwind forest edge consisting of pines and spruces. There were shrubberies of hazel below the trees; these are excluded from the simulations. In the vicinity there was a L-shaped birch grove. The ground was covered with short grass. Two microphones were used, the first placed 10 m upwind of the forest edge and the second placed at the edge close to the anemometer. A Vestas V52 wind turbine was standing at a distance of 0.8 km from the site in a 70° direction left from the mean wind direction. This might contribute to the low frequencies in the measurements.

Site 4 The location was an islet in a lake and the site contained mixed leafless aspens and birches. The vegetation area was nearly circular and surrounded by ice. The upwind distance to the lake's shore was 2.2 km with some islets between the shore and the measurement position and therefore the roughness length z_0 is

Table II. Site-specific geometry, tree height, trunk free height, anemometer, measurement position and flow-resistance values, F.

Site	H [m]	h [m]	H_a [m]	z_0 [m]	Longitude	Latitude	F [kg/s m^2]
1	12	2	10	0.4	N 60°17'2"	E 18°24'48"	$2 \cdot 10^5$
2	18	2	10	0.17	N 60°17'27"	E 18°25'15"	$2 \cdot 10^5$
3	20	2	10	0.4	N 58°30'4"	E 15°9'41"	$2 \cdot 10^5$
4	15	3	6	0.02	N 60°9'47"	E 17°18'14"	$5 \cdot 10^5$
5	20	2	6	0.07	N 60°9'47"	E 17°19'28"	$5 \cdot 10^5$
6	22	3	6	0.07	N 60°10'49"	E 17°19'6"	$2 \cdot 10^5$
7	14	2	6	0.001	N 60°10'42"	E 17°19'30"	$2 \cdot 10^5$

Table III. Site-specific meteorological parameters, temperature T, relative humidity, rh, and Turner class (TC).

Site	$T[°C]$	$rh[\%]$	TC
1	10	82	4
2	11	100	4
3	25	50	4
4	-3	60	3
5	-3	60	3
6	4	100	4
7	5	97	4

Table IV. Turbulence statistics shows wind characteristics in column **U**, sound levels, L_{pA} [dB] measured (**M**), 3D simulations (**3D**) and 2D simulations (**2D**). Average values are denoted $\bar{x}$, σ_x represents standard deviations.

		U [m/s]	**M** [L_{pA}]	**3D** [L_{pA}]	**2D** [L_{pA}]
Site 1	$\bar{x}$	5.1	50.6	52.1	51.6
	σ_x	1.7	4.0	2.8	2.2
Site 2	$\bar{x}$	6.3	45.2	49.2	49.6
	σ_x	1.5	3.0	2.1	2.8
Site 3	$\bar{x}$	5.2	56.8	59.4	56.1
Mic 1	σ_x	1.7	3.0	2.1	2.8
Site 3	$\bar{x}$	5.2	59.5	59.5	56.1
Mic 2	σ_x	1.7	5.2	1.8	3.1
Site 4	$\bar{x}$	3.2	42.2	42.6	42.2
	σ_x	0.5	3.8	2.1	2.0
Site 5	$\bar{x}$	2.6	36.0	34.8	33.7
	σ_x	0.6	3.6	1.4	1.8
Site 6	$\bar{x}$	6.8	57.0	58.2	57.5
	σ_x	1.4	3.6	1.3	2.3
Site 7	$\bar{x}$	8.3	55.4	58.7	59.1
	σ_x	1.0	2.3	1.3	2.2

difficult to estimate. The ground on the islet was frozen and covered by leaves and the understory volume contained small amounts of vegetation. The microphone was placed in the center of the islet and the anemometer was mounted 3 m from the islet's upwind edge.

Site 5 The measurement was performed on an island with leafless aspens. East of the island there was an islet. The ground on the islands was frozen and covered by leaves and the lake was covered by ice. The island had some understory vegetation of shrubberies between the ground and the canopies; these are not taken into account in the models. The microphone was placed at the island and the anemometer on the upwind edge of the main island.

Site 6 This measurement position was at an edge of leafless alders in a flooded pasture field. In the upwind direction the ground was soil without much grass or shrubberies. The mean wind direction was perpendicular to the edge.

Site 7 This vegetation area was a circular peninsula with leafless aspens and some birches. The ground was covered with a thin layer of leaves. The microphone was placed in the center of the peninsula and the anemometer at the upwind edge. In the upwind direction a lake covered with ice extended about 2 km.

4.2. Model validation

4.2.1. Prediction of spectral distributions

Comparisons between third octave band measurements and predictions from site 1–3 are shown in Figures 9 and 10. The tendency to underestimate the low frequency bands noted in section 3.3 remains, except at site 2 and site 3 microphone 2 at high wind speeds, and might be explained by the presence of noise from vegetation at longer distances or by pseudo-noise. The estimations are seen to be quite accurate, especially for site 1 and 3 but somewhat inaccurate in the compact source case, site 2 where the peak frequencies are overestimated. Possible explanations for the error at site 2 could be estimation errors either by the height or by the horizontal extensions of the tree canopies. Another possible reason could be that the wind direction was rotating from the mean wind direction causing less sheltering of the pine behind the spruce. This could increase the width of the peaks as pine needles are thicker and hence the peak frequency lower compared to spruces. A combination of the causes mentioned above is naturally also possible.

Third octave band spectra from site 4 and 7 are shown in Figure 11. The simulations for site 7 shows good agreement with measured data. The measurement from site 4 is underestimated by the model. A possible explanation for this discrepancy could be nearby islets, 0.1 km west from the site causing additional noise. This suspicion is strengthened by the favorable sound propagation conditions (stable atmospheric conditions resulting in down-

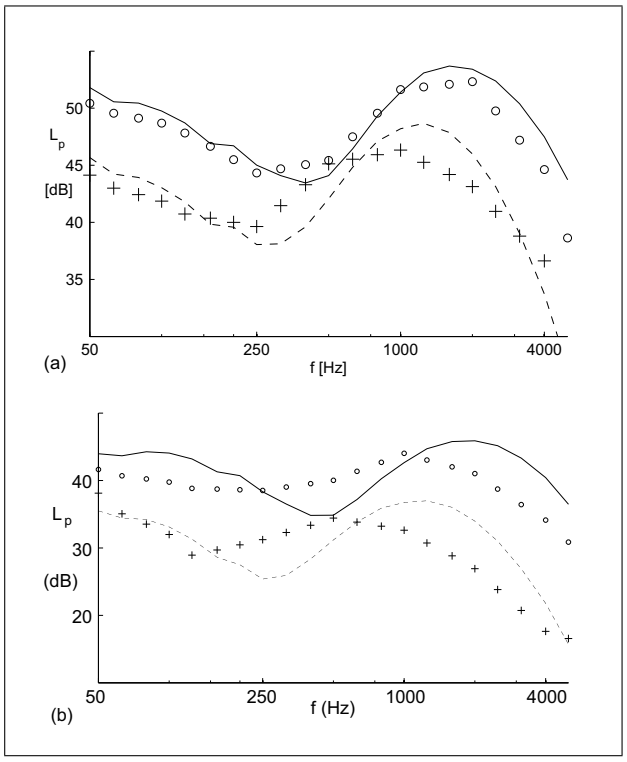

Figure 9. Third octave band spectrum of sound pressure levels. a: Site 1 at U = 8.5 m/s (∘) measurement and (—) simulation. U = 6.1 m/s (+) measurement and (- - -) simulation.
b: Site 2 at U = 8.5 m/s (∘) measurement and (—) simulation. U = 4.8 m/s (+) measurement and (- - -) simulation.

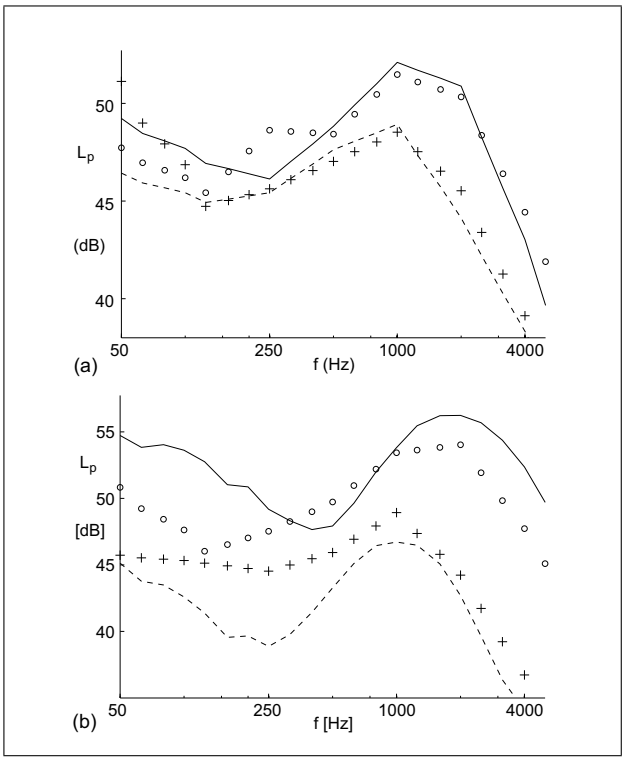

Figure 10. Third octave band spectrum of sound pressure levels. a: Site 3 Microphone 1 at U = 6.8 m/s (∘) measurement and (—) simulation. U = 4.6 m/s (+) measurement and (- - -) simulation.
b: Site 3 Microphone 2 at U = 8.3 m/s (—) (∘) measurement and (—) simulation. U = 4.6 m/s (+) measurement and (- - -) simulation.

Table V. Correlation coefficients, $R_{U,L_{pA}}$, between U and L_{pA} for measured (M), 3D simulations (3D) and 2D simulations (2D) respectively.

$R_{U,L_{pA}}$	M	3D	2D
Site 1	0.75	0.49	0.66
Site 2	0.84	0.74	0.88
Site 3 Mic 1	0.62	0.48	0.84
Site 3 Mic 2	0.59	0.46	0.88
Site 4	0.50	0.43	0.84
Site 5	0.79	0.52	0.79
Site 6	0.64	0.45	0.89
Site 7	0.77	0.75	0.78

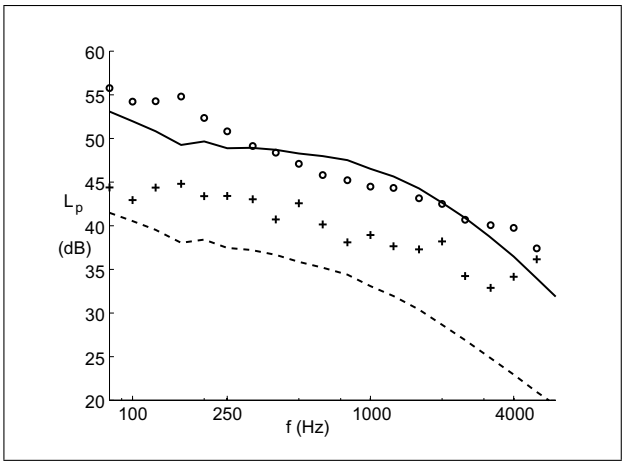

Figure 11. Third octave band spectrum from site 4 U = 3.2 m/s and site 7 at U = 6.8 m/s.

ward refraction) present during the measurements. The low correlation coefficient at site 4 compared to at the other sites, see table V, also suggests that other sources might have influenced the measurement. The measured and simulated correlation coefficients between sound pressure level and wind speed in Table V are the same order of magnitude. This indicates that the measurements are caused by the vegetation as no other sound source is present in the simulated results.

4.2.2. Characteristics of fluctuations

Earlier, two measurements of time varying vegetation noise were performed [9]. The first measurement was performed close to a shelterbelt of elms. This a tree species is not investigated in any known noise model. At a second site, consisting of aspen, spruce and pine trees, the exact vegetation geometry and meteorological data were not reported. Therefore new measurements were considered necessary in order to clarify the temporal variations of vegetation noise. Statistic properties of A-weighed sound pressure level and wind speed are shown in Table IV. In order to reduce the influence of pseudo-noise, the sound levels are A-weighed. Although the foam windscreen re-

duces the pseudo-noise this still sometimes dominates the recorded periods. These intervals are manually removed from the analyzed data. A consequence of this procedure is that some high sound levels are excluded from the analysis. However, the periods with low levels are the ones critical to the matter of masking.

Comparisons between measurements and their respective simulations are shown in Table IV. The sound levels agree well at site 1 and site 3 microphone 1. The difference at site 2 might be explained by misjudgment of the tree height and at site 3 microphone 2 by the understory vegetation that is not included in the simulation. The standard deviations of the winds are slightly underestimated by 2D and somewhat more by 3D simulations. This suggests that the 2D approximation gives satisfactory estimates of fluctuating vegetation noise.

The compact vegetation source theoretical standard deviation of sound pressure level σ_{Lp}, equation (7) proposed in [9] is computed for the second location. This is the only measurement from a compact source. equation (7) estimates a standard deviation of 6.2 dB. This is clearly an overestimation of the standard deviation in Table IV.

Measured cumulative distributions of 20-minute measurements, 2D and 3D simulations of A-weighed sound pressure levels are shown in Figure 12. The ordinates of the figures are scaled so that a straight line represents Gaussian distributions. The measured cumulative distributions are almost completely Gaussian in the intervals between 10% and 90%. Similar shapes of the distributions have been observed in the other sites. Fégeant [9] showed that large vegetation sources could be viewed as having normal distributions of sound pressure levels, which is confirmed.

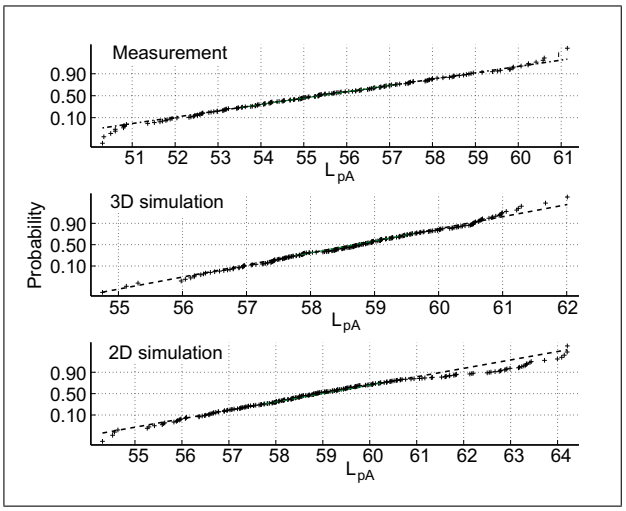

Figure 12. Cumulative distributions of A-weighed sound levels from site 7. The abscissas show L_{pA} values and ordinates show the probability. The ordinate is scaled so a Gaussian distribution is a straight line. Discrete points are shown as (+) and linear approximations as (- - -). The upper graph show measurements, the middle results from 3D simulations and the lower shows 2D simulations.

5. Discussion

The primary objective of this study was to evaluate the characteristics of vegetation-induced noise. The model developed is compared to an earlier prediction method. Improved resemblance is observed between predicted and measured spectra, particularly in the low frequency region. The deviations still present in the low frequency region between the measurements and predictions could mainly be explained by other sources of ambient noise and by the pseudo-noise caused by airflow on the microphone membrane. However, the wind tunnel measurements used to calibrate coniferous spectrum would not capture the dynamics of the large canopy elements and could therefore be responsible for a part of the errors. The model that is proposed in the paper concerning the leafless trees is, to the author's knowledge, the first of its kind and should allow for predicting vegetation noise from deciduous trees with respect to their annual changes, although intermediate states have not been investigated. The sound emission from the leafless state has been verified at only two locations. Therefore further measurements might be needed in order to adjust the parameters of this model.

A further objective of this study was to enable assessment of the masking potential of vegetation noise on wind turbine noise with higher accuracy than if turbulence is neglected. This objective is considered fulfilled as the temporal fluctuations of vegetation noise are simulated with sufficient accuracy. Models of background noise have two main advantages compared to measurements. Firstly measurements should be performed at all seasons to account for changing environmental conditions, leafed or leafless trees etc. These measurements will be time consuming and costly compared to simulations. Secondly the existence of other disturbing noise sources such as traffic noise and aircraft noise should not allow for higher noise limits from wind turbines, if these do not completely mask the wind turbine noise, otherwise the wind turbine noise will add annoyance to an already polluted environment. These negative aspects could be avoided by simulating vegetation noise instead of measuring it.

Although a general scaling law for vegetation noise derived from theoretical considerations would be very elegant the complexity and number of parameters involved seem to make this an impossible task. Nevertheless, the parametric model, originally proposed by Fégeant and further improved here, has proved to be an effective estimation technique of sound from vegetation.

Acknowledgement

The author wishes to thank Professor Mats Abom at the Marcus Wallenberg Laboratory/KTH and Associate Professor Gunilla Svensson, Department of Meteorology Stockholm University for helpful discussions. For the generous sharing of the wind field software Jakob Mann, Risø National Laboratories is gratefully acknowledged. Sandra Brunsberg, the Language Unit/KTH, is acknowledged for

proofreading. Thanks are also due to two anonymous reviewers for valuable comments. This study was supported by the Swedish Energy Agency research grant number 20134-2.

References

[1] E. Pedersen, K. P. Waye: Perception and annoyance due to wind turbine noise—a dose–response relationship. The Journal of the Acoustical Society of America **116** (2004) 3460–3470.

[2] G. P. van den Berg: Effects of the wind profile at night on wind turbine sound. Journal of Sound and Vibration **277** (2004) 955–970.

[3] J. G. McGovan, J. F. Manwell, A. L. Rogers: Wind energy explained. John Wiley & Sons, New York, 2002.

[4] O. Fégeant: Wind-induced vegetation noise. part 1: A prediction model. Acta Acustica **85** (1999) 228–240.

[5] O. Fégeant: On the masking of wind turbine noise by ambient noise. European Wind Energy Conference, EWECt'99, 1999, 184–188. Nice, France.

[6] R. M. et al.: The assessment and rating of noise from wind farms. Tech. Rept. ETSU-R-97, ETSU, Department of Trade and Industry, 1996.

[7] J. Jakobsen, T. H. Pedersen: Stoj fra vindmoller og vindstojens maskerende virkning. Tech. Rept. Lydtekniskt institut, Lyngby, 1989. Report number 141 (in Danish).

[8] O. Fégeant: Wind-induced vegetation noise. part 2: Field measurements. Acta Acustica **85** (1999) 241–249.

[9] O. Fégeant: Masking of wind turbine noise: Influence of wind turbulence on ambient noise fluctuations. Tech. Rept. 2002:12, Department of Civil and Architectural Engineering, Royal Institute of Technology, Sweden, 2002.

[10] H. Panovsky, J. Dutton: Atmospheric turbulence. John Wiley & Sons, New York, 1984.

[11] J. C. Kaimal, J. J. Finnigan: Atmospheric boundary layer flows. Oxford University Press, New York, 1994.

[12] I. N. Harman, J. J. Finnigan: A simple untfied theory for flow in the canopy and roughness sublayer. Boundary Layer Meteorology **123** (2007) 339–363.

[13] G. Raynor: Wind and temperature structure in a coniferous forest and contiguous field. Forest Sciences **17** (1971) 351–363.

[14] B. Yang, M. R. Raupach, R. H. Shaw, K. Tha, P. U, A. P. Morse: Large-eddy simulation of turbulent flow across a forest edge. part i: Flow statistics. Boundary-Layer Meteorology **120** (2006) 377–412.

[15] J. A. Businger, J. C. Wyngaard, Y. Izumi, E. F. Bradley: Flux-profile relationships in the atmospheric surface layer. Journal of the Atmospheric Sciences **28** (1971) 181–189.

[16] J. J. Landsberg, G. James: Wind profiles in plant canopies. Journal of Applied Ecology **8** (1971) 729–741.

[17] Z. Li, J. D. Lin, D. R. Miller: Air flow over and through a forest edge: A steady state numerical simulation. Boundary Layer Meteorology **51** (1990) 179–197.

[18] I. Strachan: Spatial and vertical leaf area index of a deciduous forest. Forest sciences **42:2** (1996) 176–181.

[19] M. P. Coutts, L. Grace (eds.): Wind and trees. Cambridge University Press, 1995, Ch. Modelling mechanical stresses in living sitka spruce stems, R. Milne, 165–181.

[20] M. P. Coutts, L. Grace (eds.): Wind and trees. Cambridge University Press, 1995, Ch. Turbulent airflow in forests on flat and hilly terrain, J. J. Finnigan and Y. Brunet, 3–40.

[21] B. Kruijt: Turbulence over forest downwind of an edge. Dissertation. Groningen University, 1994.

[22] B. Amiro: Comparison of turbulence statistics within three boreal forest canopies. Boundary Layer Meteorology **51** (1990) 345–364.

[23] J. Mann: Wind field simulation. Probabilistic Engineering Mechanics **13** (1998) 269–282.

[24] J. C. Kaimal, J. C. Wyngaard, Y. Izumi, O. R. Coté: Spectral characteristics of surface-layer turbulence. Quarterly Journal of the Royal Meteorological Society **98** (1972) 563–589.

[25] J. Mann: The spatial structure of neutral atmospheric surface-layer turbulence. Journal of fluid mechanics **274** (1994) 141–168.

[26] ISO/DIS 9613-1: Attenuation of sound during propagation outdoors – Part 1: Atmospheric absorption. International Organization for Standardization, Geneva, Switzerland, 1995.

[27] M. E. Delany, E. N. Bazley: Acoustical properties of fibrous absorbant materials. Applied Acoustics **3** (1970) 105–116.

[28] J. Kragh et al.: Nordic environmental noise prediction methods. nord2000. Tech. Rept. 1719/01, Delta Acoustics, Lyngby, 2001.

[29] ISO/DIS 9613-2: Attenuation of sound during propagation outdoors – Part 2: General method of calculation. International Organization for Standardization, Geneva, Switzerland, 1996.

[30] A. Tunick: Calculating the micrometeorological influences on the speed of sound through the atmosphere in forests. J Acoust Soc Am **114** (2003) 1796–1806.

[31] O. Fégeant: Wind turbine noise assessment. Tech. Rept. Building Acoustics, KTH, Stockholm, 1997. TRITA-BYT 97/175.

[32] P. Zeng, H. Takahashi: A first order closure model for the wind flow within and above vegetation canopies. Agricultural and Forest Meteorology **103** (2000) 301–313.

[33] B. Marklund: Biomassafunktioner för tall, gran och björk i sverige. slu, institutionen för skogstaxering (biomass functions for pine, spruce and birch in sweden). Tech. Rept. 45, Sveriges Lantbruksuniversitet, 1988. (in Swedish).

[34] T. Johansson: Increment and biomass in 20- to 91-year-old european aspen and some practical implications. Biomass and Bioenergy **23** (2002) 245–255.

[35] T. Johansson: Dry matter amounts and increment in 21- to 91-year-old common alder and gray alder and some practical implications. Canadian Journal of Forrest Research **29** (1999) 1679–1690.

[36] Noise from offshore wind turbines. Danish Environmental Protection Agency, 2005. Environmental Project no. 1016.

[37] ISO1996: Acoustics - Description and measurement of environmental noise. International Organization for Standardization, Geneva, Switzerland, 1986.